〈論文〉 4-5-11

'99 전력전자학술대회 우수추천논문

전동기 과전압 억제용 OUTPUT REACTOR의 최적 설계

金 翰 鍾, 李 根 浩, 張 喆 浩, 李 濟 弼

Cost-effective Design of an Inverter Output Reactor in ASD application

Han-Jong Kim, Geun-Ho Lee, Cheol-Ho Jang, Jea-Pil Lee

요 약

본 논문은 전동기 과전압 억제용으로 사용되는 인버터 출력 리액터의 최적 설계 방식을 제시하고 있다. 전력선의 길이가 상대적으로 짧은 엘리베이터 구동 시스템의 인버터 출력단에 리액터를 사용하는 경우, 전동기 선간의 과 전압 특성은 과 진압 동작 주파수인 상당한 고 주파수 대역에서의 출력 리액터와 전동기 특성에 의해 좌우된다. 따라서, 고 주파수 대역에서의 출력 리액터 및 전동기의 동작 특성을 분석하고, 출력 리액터의 필요 파라미터를 추출하였다. 이를 리액터의 설계 변수하고, 리액터의 고 주파수 특성을 고려하여, 새로운 구조의 출력 리액터 설계방식을 제안하였다. 통상의 출력 리액터와 제안된 방식의 출력 리액터를 용량 15kW급의 엘리베이터 유도 전동기 구동 시스템에서 비교 실험하여, 제안된 방식의 효과를 검증하였다.

ABSTRACT

In this paper, the cost-effective design of output reactor which is used to suppress the over-voltage at the motor terminal in the Adjustable Speed Drives(ASD) application is proposed. In the elevator drive system, the power cable length is relatively shorter than other ASD applications and then the over-voltage at the motor terminal depends on the frequency characteristics of the output reactor at the over-voltage operating frequency. The over-voltage suppression mechanism of output reactor in ASD application is analyzed and the dominant parameters of output reactor for the over-voltage suppression are extracted. Using these parameters as the design values and considering the high frequency characteristics of iron core in the reactor, a new cost-effective structure of output reactor is proposed. Experimental results of the conventional reactor and the proposed reactor with a 15kW induction motor are given to verify the proposed scheme.

Key Words : output reactor, ASD application, over voltage suppression

1. Introduction

Recent advancements in power electronic switching devices have enabled high frequency switching operation and have improved the performance of ASD. While the high switching speed improved the performance of the inverter-fed motors, the high rate of voltage-rise in inverter output arises the excessive over-voltage in the motor terminal, which has serious adverse effect on the motor insulation [1] [3]. The over-voltage at the motor terminal is clearly analyzed with the voltage reflection theory for the cable end which explains that the voltage overshoot depends on the inverter output voltage rise-time, cable length, and the reflection coefficient of the cable end [4], [5]. Many papers propose various methods to solve this problem, and the output reactor at the inverter is the simplest method of

conditioning the motor terminal voltage[6] [8]. The output reactor reduces the dV/dt of inverter output voltage, which in turn reduces the dV/dt of the motor terminal voltage. In general, output reactor is designed at the fundamental frequency, having 3~5% Percent Impedance and the over-voltage suppression is almost proportional to the reactor impedance. But a higher value of impedance causes a rapid increase in cost. In the conventional reactor design, to extract the optimal parameter of the output reactor, the trial and error method is used, but this empirical way takes much time and high cost. Besides, a higher value of impedance at fundamental frequency causes a larger voltage drop across the reactor, which reduces the fundamental component of voltage at the motor terminals. In the elevator drive, the acceleration torque is larger than that of others and then a large voltage drop can result in the torque insufficiency. In this paper, we analyze the over-voltage suppression mechanism of output reactor and it is found that the over-voltage suppression performance of the output reactor depends on the certain parameters at over-voltage operating frequency. At several hundreds of kHz (over-voltage operating frequency), the magnetic penetration depth of reactor core is reduced and the flux distribution is different from that of the fundamental frequency. Using these characteristics, we propose a cost-effective design of output reactor.

2. Over-voltage suppression mechanism of output Reactor

Fig. 1 shows the motor driving system with output reactor. The output reactor is implemented at the inverter output. Fig. 2 shows the voltage measured at the motor terminal. Fig. 2 (a) shows the voltage when the motor cable end(the neutral of Y-connection motor) is opened, and Fig. 2 (b) shows the voltage when the motor cable end is shorten. The results show that the over voltage characteristic is almost independent of the magnitude of the fundamental current.

Fig. 3 shows the voltage and current measured at the motor terminal. The current waveform has the frequency characteristic which ranges several hundreds of kHz. This shows that the high frequency modelling of the system (motor, power cable, and output reactor) must precedes the voltage suppression mode analysis.

2.1 Motor model at high frequency

Many papers show various ways of the high frequency motor modelling. In this paper, the way of Takamasa Hori is used[9]. Fig. 4 shows the Impedance vs frequency characteristic of the tested motor(7.5kW). The impedance characteristics of each phase coil of the motor is measured with Impedance Analyzer(HP4194A). Fig. 5 shows the motor equivalent circuit for the single phase, and Table 1 shows the calculated parameter of the given circuit.

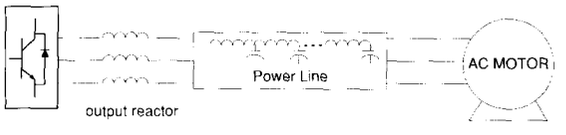

Fig. 1 Motor driving system

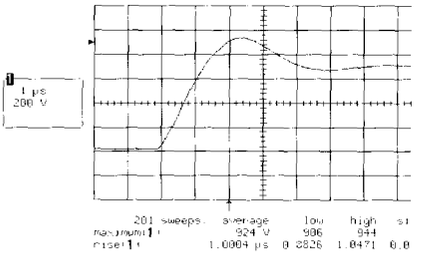

(a) No fundamental current
(when motor neutral is opened)

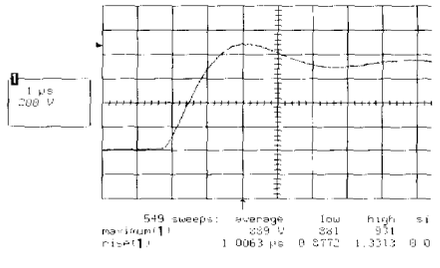

(b) Rated current
(when motor neutral is shorted)

Fig. 2 The voltage measured at the motor terminal

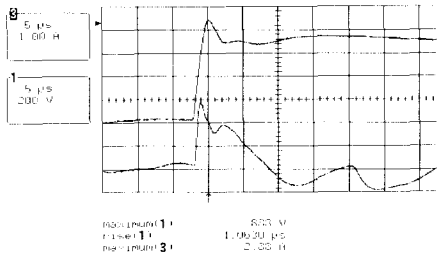

Fig. 3 The voltage and the current measured at the motor terminal (Ch1 : voltage, Ch3 : current, motor neutral is opened)

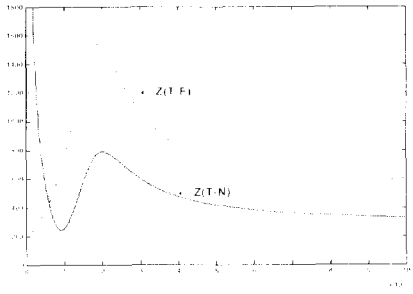

Fig. 4 The impedance characteristics of the motor

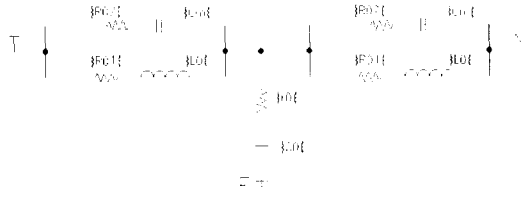

Fig. 5 The high frequency equivalent circuit of motor (single phase)
(T:input terminal, N:neutral, F:Frame ground)

Table 1 The calculated parameters

R01	80.3 ohm
R02	272 ohm
Lo	367 uH
Cm	2.1 nF
ro	27.7 ohm
Co	4.7 nF

2.2 Reactor model at high frequency

Fig. 6 shows the output reactor circuit for the single phase, and Table 2 shows the measured parameters of the given circuit. Impedance Analyzer (HP4194A) is used in measuring.

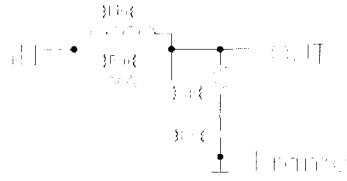

Fig. 6 The high frequency equivalent circuit of reactor (single phase)

Table 2 The measured parameters

Lin	76 uH
Rin	293 ohm
Rp	90 ohm
Cp	40 pF

2.3 The analysis of the over-voltage suppression mechanism.

In the elevator application, the power cable-length is less than 20[m]. If the output reactor increases the voltage rise time, the effect of power cable can be ignored. Fig. 7 shows the total system where the high frequency model of the previous chapter is used. Fig. 8 shows the Pspice simulation results. The rise-time of input voltage(Vin) is 100nsec. The voltage overshoot at motor terminal depends on the current I(tot) into the motor terminal which is divided into two currents, I(L), I(C). Fig. 8 shows that the current I(C) is dominant at the voltage transient, and then it is found that the Lo and R01 path in Fig. 7 can be ignored in the voltage overshoot concern. Then, at the over voltage operating frequency(ωtyp), the total system can be simplified into the circuit in Fig. 9 As a result, the design of output reactor for over voltage suppression is simplified into the step response design of R L C series resonant circuit, that is, finding the Rs and Ls parameter for the desired voltage response.

In Fig. 9,

$$R_s = \frac{(w_{typ}L_{in})^2 R_{in}}{R_{in}^2 + (w_{typ}L_{in})^2} \quad (1)$$

$$L_s = \frac{L_{in}R_{in}^2}{R_{in}^2 + (w_{typ}L_{in})^2} \quad (2)$$

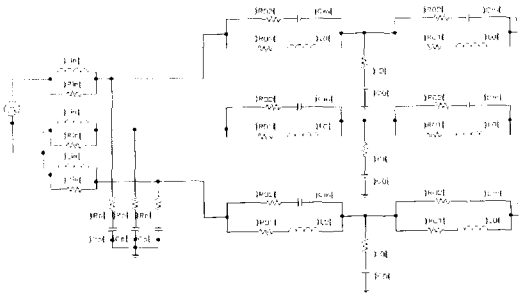

Fig. 7 The system model at the high frequency

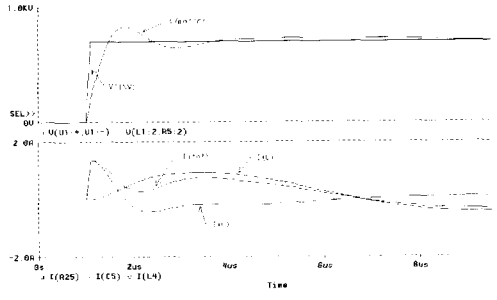

Fig. 8 The Pspice simulation result
I(tot):total current, I(C):current in Cm,
I(L):current in Lo

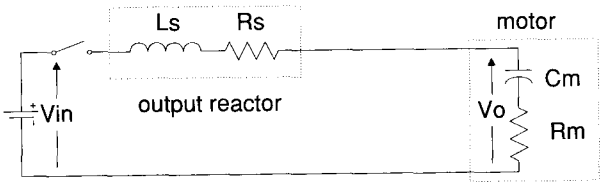

Fig. 9 The simplified system

The transfer function of the simplified system is

$$\frac{V_o}{V_{in}} = \frac{R_m C_m s + 1}{L_s C_m s^2 + (R_s + R_m) C_m s + 1} \tag{3}$$

Then, the characteristic equation of the system is

$$\Delta = s^2 + \frac{R_s + R_m}{L_s} s + \frac{1}{L_s C_m} = 0 \tag{4}$$

In the general second order system,

$$\Delta = s^2 + 2\xi w_n s + w_n^2 = 0 \tag{5}$$

Then,

$$\xi = \frac{R_s + R_m}{\sqrt{4L_s/C_m}}, \quad w_n = \frac{1}{\sqrt{L_s C_m}} \tag{6}$$

In Eq. (6), ξ is the damping ratios and ωn is the natural frequency. From Eq. (6), we can find that the increase of Rs makes the increase of damping ratio and that the increase of Ls makes the decrease of the damping ratio, and the natural frequency.

Fig. 10 shows the characteristics of the voltage overshoot with the variance of Rs and Ls. Fig. 10 (a) shows that the voltage overshoot decreases when Rs increases, and Fig. 10 (b) shows that the natural frequency decreases when Ls increases.

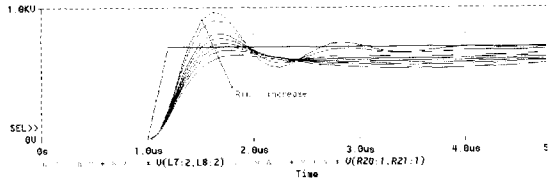

(a) When Rs increases

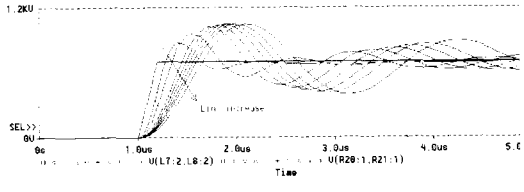

(b) When Ls increases

Fig. 10 The voltage overshoot at the motor terminal

3. Design of Output Reactor

From the previous chapter, it is expected that the over-voltage suppression characteristics of output reactor depends on Ls and Rs parameters at the over-voltage operating frequency(ω_{typ}). Then the over-voltage suppression design becomes the design of output reactor having the required Ls and Rs parameters at over-voltage operating frequency(ω_{typ}). Ls and Rs depend on the flux linkage and the core loss inside the reactor which are related to the

flux distribution inside the reactor core. The reactor design considerations for the over-voltage suppression are as following.

3.1 The effect of core Saturation

If the saturation arises inside the reactor, Ls and Rs values of the reactor are changed. Then, the over voltage suppression characteristics of output reactor is also changed. Fig. 11 shows the voltage overshoot at the motor terminal when the current is (a) 40Arms and (b) 80Arms. The inductance of the used reactor is 0.35mH when 40Arms flows but decrease to 0.27mH when 80Arms because of core saturation. In Fig. 11 (b), it is found that the voltage overshoot becomes higher and the voltage rise time decreases, which shows the effect of the core saturation. From this result, it is found that the iron core of output reactor must not be saturated even when the maximum current flows. This causes the increase of the cost and the size of the output reactor.

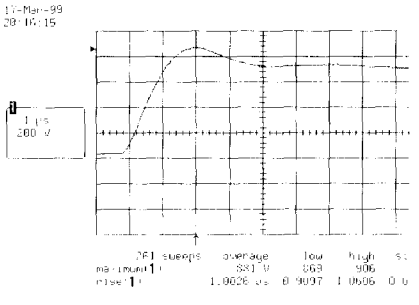

(a) 40Arms(0.35mH)

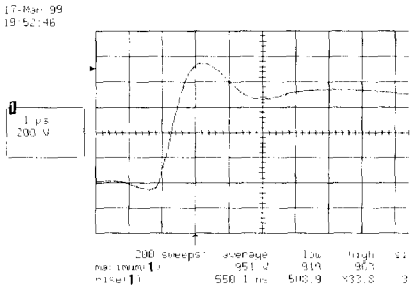

(b) 80 Arms(0.27mH, saturated)

Fig. 11 The motor terminal voltages at different currents

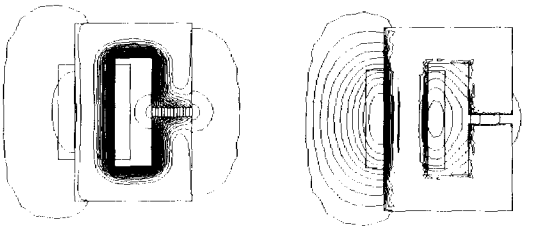

(a) 60Hz (b) 200kHz

Fig. 12 The flux distribution at the different frequency

3.2 The Flux distribution in high frequency

When the current produces a magnetic field(Ho) and a flux density(Bo) in the core walls, the flux penetration into the iron core laminations is given by one dimension diffusion equation [10].

$$\frac{d^2B}{dx^2} - \frac{j}{p^2} = 0 \tag{7}$$

where $p = \sqrt{\frac{\rho}{\mu\,\omega}}$

p =Penetration depth
ρ =Iron resistivity
μ =Iron permeability
ω =Angular frequency
χ =Distance

The solution for Eq.(7) is given

$$B(x,\omega) = B_o \exp(-\frac{x}{p}) \tag{8}$$

According to Eq.(8), the flux penetration depth in reactor core decreases rapidly, when the source frequency increases. Fig. 12 shows the flux distribution in the core, when the current frequency is (a) 60Hz, and (b) 200kHz. F.E.M(finite element method) is used for the analysis of the flux distribution.

The single phase reactor structure is adopted, and the lamination effect is neglected for the convenience of the analysis. Although there can be some deviations because of this simplification, the approximate trends can be found. The flux leakage at high frequency (Fig. 12 (b)) is more apparent

than that at low frequency (Fig. 12 (a)).

3.3 Cost-effective design of output reactor

In the large inertia system like the elevator, the current for acceleration is more than two times of the rated current. If the closed yoke type reactor is adopted in this application, it causes a great increase in the cost to avoid the over-current saturation problem. Fig. 13 shows the design concept of the proposed output reactor structure. Fig. 13 (a) hows the low frequency flux distribution in conventional closed yoke type where the flux is equally distributed in the whole core.

Fig. 13 (b) shows the flux distribution at the high frequency where the flux leakage is dominant. Fig. 13 (c) shows the proposed open yoke type structure which also has the similar flux distribution with that of conventional type in Fig. 13 (b). It is expected that the over-voltage suppression characteristics will be similar because their flux distributions are similar at the over-voltage operating frequency. Having the same over-voltage suppression characteristics, the open yoke type has some merit beyond the closed yoke type. In low frequency, the open yoke type reactor has lower flux density than the closed type, which can reduce the size and the cost of reactor without the saturation problem. Fig. 14 shows the proto-type of the proposed structure (single lag). Fig. 15 shows the two different types of 3 phase reactors which are designed for the similar over-voltage suppression characteristics. Table 3 shows the design results of two different type reactors in Fig. 15 At 60Hz, the inductance of the proposed reactor is smaller than that of conventional type, and then the voltage drop across the inductor becomes smaller. This will increase the available torque range. Fig. 16 shows the measured Ls and Rs values of two reactors. It is found that two reactors have similar characteristics in the over-voltage operating frequency (200kHz ~ 500kHz). Fig. 17 shows the voltage at the motor terminal when the reactor at inverter output is (a) the conventional type and (b) the proposed type. For the accuracy, the statistical analysis using more than 200 samplings are accomplished.

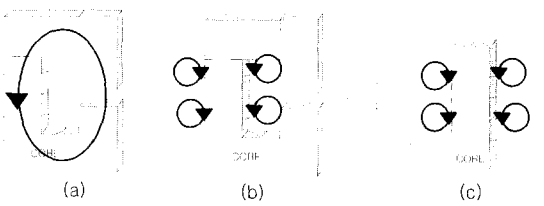

Fig. 13 The flux distribution in output reactor

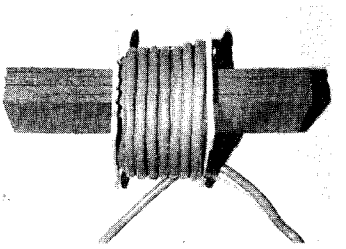

Fig. 14 Proto-type of the proposed output Reactor (single Leg)

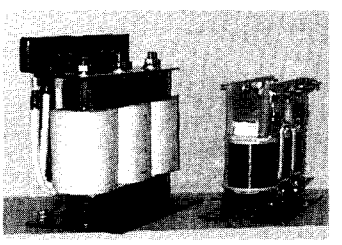

Fig. 15 The conventional type and the proposed type

Table 3 The specification of two reactors in Fig. 15 (Inductance are measured at 60Hz)

Item	conventional	proposed
Rated current	55 Arms	55 Arms
Rated inductance [mH] (at rated current)	0.25	0.185
Overload Inductance [P.U.] (at 200% current)	89.8% of rated value	89.3% of rated value
Core size(W*H*D[mm])	220*160*40	160*110*40
Total weight [Kg]	10.5	4.5

Table 4 shows these results. Although the overall voltage characteristics are similar, there are small differences in values. We can guess that the

differences are due to the parameter difference of two reactors. Smaller Ls value and larger Rs value of the conventional type cause the increase of the damping ratio and the decrease of the natural frequency.

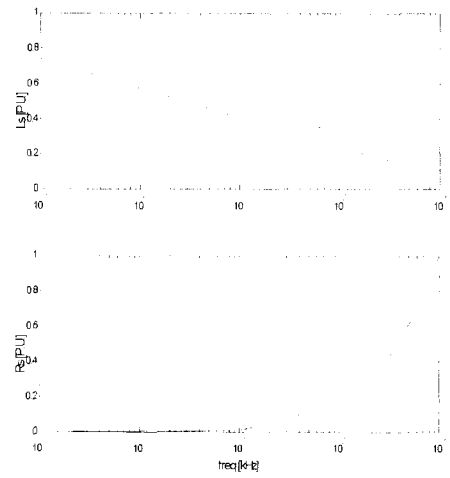

Fig. 16 The Ls and Rs vs. the frequency [P.U.]
(Dashed:conventional, Continuous line:proposed)

Table 4 The voltage overshoot measured at the motor terminal (when DC Link voltage is 540Vdc)

Item	Conventional		Proposed	
	Average	variance	Average	variance
the max.voltage[V]	636	10	667	15
rise time [usec]	451	7	490	35

4. Conclusions

In this paper, the cost-effective design of output reactor which is used to suppress the over-voltage at the motor terminal in ASD application has been proposed. And the open yoke structure which needs smaller core size than the conventional closed yoke type has been proposed.

From the analysis of over-voltage suppression mechanism, it was found that the over-voltage suppression performance of the output reactor depends on certain parameters at the over-voltage operating frequency and that the flux leakage is dominant at that frequency. The Ls and Rsparameters which are dominant in over voltage

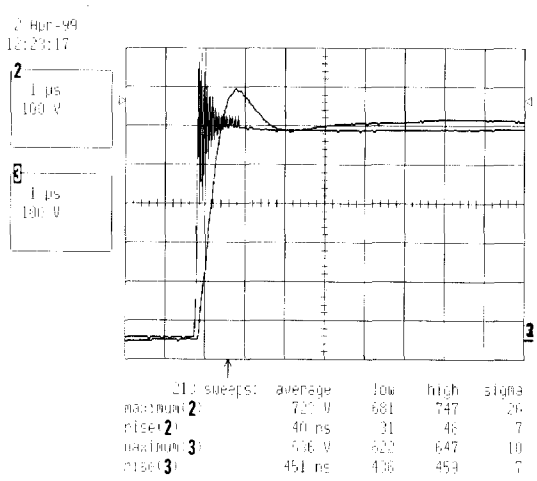

(a) conventional

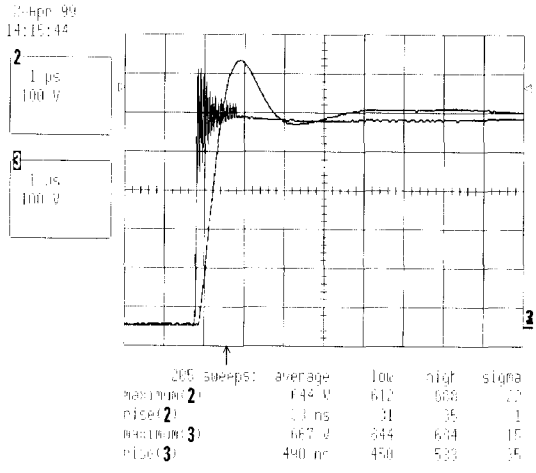

(b) proposed

Fig. 17 The voltage-overshoot at the motor terminal
(Ch2: the voltage at reactor input,
Ch3: the voltage at motor terminal)

suppression was adopted as the design values of the reactor. And the open yoke structure which needs smaller core size than the conventional closed yoke type has been proposed.

Experiments of the conventional reactor and the proposed reactor with a 15kW induction motor showed the similar results, which verifies the proposed scheme. In elevator application(15kW), the size and the weight in the proposed design can be reduced to about a half of those in the conventional.

Reference

[1] E.Persson, "Transient Effects in Apllication of PWM Inverters to Induction Motors," IEEE Trans. Ind.Appl., Vol .28. No. 5, pp. 1095~1101.

[2] G.Skibinski, J.Erdman, J. Pankau and J. Campbell, "Accessing AC Motor Dielectric Withstand Capability to Reflected Voltage Stress using Corona Testing," Thirty-First IAS Annual Meeting, IAS '96., Conference Record of the 1996 IEEE Volume : 1, pp. 694~702.

[3] Austin H. Bonnett, "A Comparison Between Insulation Systems Available for PWM Inverter Fed Motors," IEEE Trans. Ind.Appl., Vol. 33, No. 5, Sep/Oct 1997, pp. 1331~1341.

[4] Mike Melfi, Jzson Sung, Sid Bell and G.Skibinski, "Effect of Surge Voltage Risetime on the Insulation of Low Voltage Machines Fed by PWM Converters," Thirty-Second IAS Annual Meeting, IAS '97, Conference Record of the 1997 IEEE Volume : 1, pp. 239~246.

[5] R.Kerkman, D.Leggate and G.Skibinski, "Interaction of Dive Modulation & Cable Parameters on AC Motor Transient," Thirty-First IAS Annual Meeting, IAS '96., Conference Record of the 1996 IEEE Volume 1, pp. 143~152 .

[6] Paul T.Finlayson, "Output Filters for PWM Drives with Induction Motors," IEEE Ind.Appl Magazine, Jan/Feb 1998, pp. 45~52.

[7] Annette von Jouanne and P.Enjeti, "Design Considerations for an Inverter Output Filter to Mitigate the Effects of Long Motor Lead in ASD Applications," IEEE Trans. Ind.Appl., Vol. 33, No. 5, Sep/Oct 1997, pp. 1138~1145.

[8] G.Skibinski, "Design Methodology of a Cable Terminator to Reduce Reflected Voltage on AC Motors," Thirty-First IAS Annual Meeting, IAS '96., Conference Record of the 1996 IEEE Volume : 1, pp. 153~161.

[9] T. Hori, "High frequency Zero Phase Sequence Equivalent Circuit of Induction Motor Driven by PWM Inverter," TIEE Japen Vol. 116-D, No. 10 1996.

[10] J.L Guardado and K.J.Cornick, "Calculation of Machine Winding Electrical Parameters at High Frequencies for Switching Transient Studies," IEEE Trans. Energy Conversion, Vol. 11, No. 1, March 1996, pp. 33~40.

저 자 소 개

김한종(金翰鍾)

1970년 6월 11일생. 1994년 한양대 공대 전기공학과 졸업(학사). 1996년 동 대학원 전기공학과 졸업(석사). 1996년~현재 LG산전 빌딩시스템연구소. 주임 연구원.

이근호(李根浩)

1969년 4월 11일생. 1992년 한양대 공대 전기공학과 졸업(학사). 1994년 동 대학원 전기공학과 졸업(석사). 1994년~현재 LG산전 빌딩시스템연구소. 선임 연구원.

장철호(張喆浩)

1963년 3월 2일생. 1988년 부산공업대 전기공학과 졸업(학사). 1995년 부산 대학원 전기공학과 졸업(석사). 1988년~현재 LG산전 빌딩시스템연구소. 책임 연구원.

이제필(李濟弼)

1964년 4월 17일생. 1987년 건국대 공대 전기공학과 졸업(학사). 1989년 동 대학원 전기공학과 졸업(석사). 1989년~현재 LG산전 빌딩시스템연구소. 책임 연구원.